Electric Power Systems Research 154 (2018) 204–212

Contents lists available at ScienceDirect

Electric Power Systems Research

journal homepage: www.elsevier.com/locate/epsr

Parameters estimation of three-phase induction motors using differential evolution

Jacqueline Jordan Guedes, Marcelo Favoretto Castoldi, Alessandro Goedtel*, Cristiano Marcos Agulhari, Danilo Sipoli Sanches

Federal University of Technology – Paraná, 86300-000 Cornélio Procópio, PR, Brazil

ARTICLE INFO

Article history:
Received 28 April 2017
Received in revised form 25 August 2017
Accepted 26 August 2017

Keywords:
Induction motor
Differential evolution
Parameters estimation

ABSTRACT

Three-phase induction motors are extensively used in the industry due to their robustness characteristics, low cost and easy maintenance. Usually, it is necessary to implement drive and control systems for such motors, which requires the knowledge of their mechanical and electrical parameters. However, in some cases, these data are not immediately available, or the values of the parameters may change due to the wear of motor components. Such problems can be circumvented if an efficient parameter estimation technique is available. In order to automatically estimate the parameters efficiently, the present work proposes a method, based on the differential evolution algorithm, aimed at the estimation of the electrical and mechanical parameters of three-phase induction motors. Such algorithm is capable of estimating the parameters of the equivalent electrical circuit, such as stator and rotor resistances and leakage inductances, the magnetizing inductance, and also mechanical parameters, such as moment of inertia and the friction coefficient. The performance of the proposed parameter estimation technique is evaluated for three different input signals: (i) current signal of a phase associated with the speed measured from a tachogenerator, (ii) current signal of a phase associated with the speed acquired from a torquemeter, and (iii) only the current signal of one phase. Finally, a series of simulated and experimental results are presented to validate the proposed technique, and the results show the good performance of the proposed strategies.

1. Introduction

Three-phase induction motors (TIM) are widely used in the industrial sector, mainly for the operation of pumps, compressors and fans, representing 68% of the Brazilian industrial energy consumption, which corresponds to 35% of the total consumed electrical energy [1]. In general, such motors operate under approximately 60% of their nominal load, consequently working with reduced efficiency, which results in energy waste [2,3].

The efficiency graph of a TIM, for the nominal frequency, can be found in its datasheet. However, these motors are often driven by frequency inverters, resulting in operating frequencies different from their nominal values. One way of analyzing TIM efficiency, and consequently of defining which operating region is more appropriate for a given situation, is to perform calculations that depend on the electrical and mechanical parameters of the motor, since such parameters, when applied to a mathematical model, may represent the operating dynamics of the TIM [4]. However, in several situations the parameters may not be informed by the manufacturer, or external and internal influences, such as electrical and mechanical wear or heating [5], may modify the values of the parameters. In addition to problems related to energetic efficiency, a proper estimation of the TIM parameters may influence the AC drives performance, since the values of the motor parameters are fundamental for controller tuning [6–8], especially the mechanical parameters, which are related to the dynamic response during the transient [9]. Even fault diagnosis methods can be accomplished by monitoring the parameters of a TIM [10]. In this context, the development of techniques for the estimation of the electrical and mechanical parameters of TIM has become an important topic of recent researches.

The data for the symmetric equivalent electrical circuit are typically obtained through blocked and no-load rotor experiments, as stated in the IEEE norm [11], where the machine operates under steady state. Although such method is simple and commonly used, its approximation may not be precise. Additionally, the mechan-

* Corresponding author.
E-mail address: agoedtel@utfpr.edu.br (A. Goedtel).

http://dx.doi.org/10.1016/j.epsr.2017.08.033
0378-7796/

ical parameters are not estimated in this approach. In this sense, computational methods rise as attractive alternatives, due to their capability of yielding more precise estimations of both electrical and mechanical parameters.

In [12] two methods are proposed to calculate the equivalent electrical circuit parameters. The methods are respectively based on Artificial Neural Networks (ANN) and Adaptive Neuro-Fuzzy Inference Systems (ANFIS), and the input data are the torque, active and reactive power, starting current, maximum torque, full load speed and efficiency, given by the manufacturer. The technique proposed in [13] is based on the use of the Adaline network to identify the rotor time constant and the leakage factor of the TIM under steady state (high frequencies), as well as the leakage resistance and inductance of the stator (low frequencies). In [14] the use of variable frequency tests on the computation of the equivalent electrical circuit parameters is also proposed.

In the last years, estimation techniques for electrical and mechanical parameters of TIM, based on the use of computational methods, have been reported in the literature with interesting results. For instance, the work in [15] proposes the identification of the moment of inertia of the TIM using only a voltage sensor, which is modeled in terms of the parameters to be estimated, resulting in a simple and low cost technique. The use of online parameters estimation algorithms is also proposed in [16], which consists of a predictive control technique based on an Euler approximation to estimate the stator resistance from the induction motor linear model. In [17], a Particle Swarm Optimization (PSO) technique is applied to the estimation of the equivalent electrical circuit parameters of TIM, comparing the torque and the specifications provided by the manufacturer.

Another class of heuristic computational methods is the class of evolutive algorithms, which are based on defining and changing populations of solutions to minimize an objective function. The application of evolutive algorithms in the TIM parameters estimation has also been reported on the recent literature. In [18], the use of genetic algorithms to simultaneously identify mechanical and electrical parameters is proposed, using as input only the corresponding starting current and voltage. The method proposed in [19] consists of using the Differential Evolution (DE) algorithm to estimate the rotor and stator resistances, as well as the rotor and stator leakage inductances, by comparing the nominal, starting and stop measured torques with the values resultant from the estimated parameters. In [20], the influence of the temperature variation of the electrical and mechanical parameters of TIM using only a current signal is analyzed. Additionally, in [21] the authors propose the analysis of five different DE approaches to verify which is the best parameter estimation technique for the equivalent electrical circuit of TIM, by using simulated signals of three-phase input and output voltages. Finally, in [22] the DE is used to estimate the parameters of the equivalent electrical circuit and of the moment of inertia, considering as input signal the simulated three-phase currents of two different motors.

In a general analysis, the main difficulty reported on some of the proposed methods is the acquisition of the necessary information for the parameter identification, as speed and torque [12,17,19]. Such papers use more sophisticated sensors, implying higher costs of developing the project and consequently decreasing their attractiveness. Besides, the presented methods propose alternatives for the parameters estimation of either the TIM equivalent electrical circuit [12,14,17,21] or the mechanical parameters [15], instead of considering their combination. The works presented in [18,20,22] propose approaches for the estimation of both electrical and mechanical parameters. However, the method in [18] requires the three-phase voltage and current data, consequently demanding six sensors, and [20] uses only computational data.

In the present paper, we propose a technique capable of estimating the values of the rotor and stator resistances and leakage inductances, the magnetizing inductances (parameters of the equivalent electrical circuit), moment of inertia and friction coefficient of the three-phase induction motor. Three distinct sets of input signals are applied to the proposed algorithm: (i) current signal of one phase along with the speed measured from a tachogenerator, (ii) current signal of one phase along with the speed measured from a torquemeter, and (iii) only the current signal of one phase. The method consists of a function approximator for parameter estimation using the Differential Evolution algorithm, combined with the TIM dynamical model, as described in [23,24]. In order to verify the efficiency and validate the proposed estimation method, tests based on computational models executed with experimental data were also performed.

2. Three-phase induction motor modeling

The mathematical modeling of the induction motor is essential for the parameters estimation approach proposed in this paper. In fact, the evaluation of a given set of parameters in the present method is performed through the numerical simulation of the induction motor dynamics, whose mathematical model depends on the parameters to be evaluated, followed by a comparison of the simulated results with the experimental data. In this paper, the linear model of the motor is considered, since it is supposed to operate at no-load and, consequently, the saturation region can be neglected. The detailed induction motor modeling can be found in [23,24].

The motor model consists of voltage and current equations from the rotor and stator, flux of the rotor and stator, electromagnetic torque and angular position.

A unique referential is adopted for the rotor and stator, which can be stationary or synchronous. In this work, the only referential adopted is the stationary one, since the measured values refer to the stator.

The voltage and current equations of the rotor and stator are described in (1) and (2), sub-index 1 refers to the stator quantities and sub-index refers 2 to the rotor.

$$\underline{u}_1 = R\underline{i}_1 + \frac{\mathrm{d}}{\mathrm{d}t}\underline{\Psi}_1 \tag{1}$$

$$\underline{u}_2 = 0 \tag{2}$$

On matrix form, Eqs. (1) and (2) are rewritten as (3) and (4):

$$\begin{bmatrix} u_{1a} \\ u_{1b} \\ u_{1c} \end{bmatrix} = R_1 \begin{bmatrix} i_{1a} \\ i_{1b} \\ i_{1c} \end{bmatrix} + \frac{d}{dt}\left(L_1 \begin{bmatrix} i_{1a} \\ i_{1b} \\ i_{1c} \end{bmatrix} + L_H \begin{bmatrix} i_{2a} \\ i_{2b} \\ i_{2c} \end{bmatrix} \right) \tag{3}$$

$$R_2 \begin{bmatrix} i_{2a} \\ i_{2b} \\ i_{2c} \end{bmatrix} + \frac{d}{dt}\left(L_2 \begin{bmatrix} i_{2a} \\ i_{2b} \\ i_{2c} \end{bmatrix} + L_H \begin{bmatrix} i_{1a} \\ i_{1b} \\ i_{1c} \end{bmatrix} \right) = 0, \tag{4}$$

where R_1 and R_2 are the stator and rotor resistances (Ohm), $\underline{i}_1$ and $\underline{i}_2$ are the three-phase currents from stator and rotor (Ampere), $\underline{u}_1$ and $\underline{u}_2$ are the three-phase voltages from stator and rotor (Volts), $\underline{\Psi}_1$ and $\underline{\Psi}_2$ are the flux from the stator and rotor (Weber), respectively.

The equations for the stator and rotor fluxes are given by (5) and (6),

$$\underline{\Psi}_1 = L_1\underline{i}_1 + L_H\underline{i}_2 = L_H(\underline{i}_1 + \underline{i}_2) + l_{\sigma 1}\underline{i}_1 \tag{5}$$

$$\underline{\Psi}_2 = L_1\underline{i}_2 + L_H\underline{i}_1 = L_H(\underline{i}_2 + \underline{i}_1) + l_{\sigma 2}\underline{i}_2 \tag{6}$$

L_1 and L_2 defined as

$$L_1 = L_H + l_{\sigma 1}, \;\; L_2 = L_H + l_{\sigma 2}. \tag{7}$$

The variables L_1 and L_2 are the stator and rotor total inductances, respectively, $l_{\sigma1}$ and $l_{\sigma2}$ are the leakage inductances of the stator and rotor, respectively, and L_H is the magnetizing inductance. All the inductances are measured in Henry.

Based on the flux and current values computed in (2)–(6), the electromagnetic torque can be calculated by (8)

$$m_d = -P\underline{\Psi}_1^T \underline{K} \underline{i}_1, \tag{8}$$

where P is the number of poles pairs and $\underline{K}$ represents the transformation matrix for the unique referential, given by (9):

$$\underline{K} = \frac{1}{\sqrt{3}} \begin{bmatrix} 0 & -1 & 1 \\ 1 & 0 & -1 \\ -1 & 1 & 0 \end{bmatrix} \tag{9}$$

To complete the model, the electromagnetic torque is inserted in the mechanical equation and is denoted by

$$J\frac{d}{dt}\omega_{mec} = m_d - K_D\omega_{mec} - m_l \tag{10}$$

where J is the inertia moment (kg m^2), ω_{mec} is the motor speed (rad/s), m_l is the load torque (N m), m_d is the electromagnetic torque (N m) and K_D is the friction coefficient. When the motor is at no-load operation and at constant speed, Eq. (10) can be simplified, allowing the calculation of the friction coefficient by

$$K_D = \frac{\omega_{mec}}{m_d} \tag{11}$$

In this work, a series of no-load tests were performed for the parameters estimation, in order to identify the friction coefficient. Using the presented equations, it is possible to develop a state space model, in which the states are given by the currents and speed.

The DE algorithm, developed in this paper, is presented in Section 3. The optimization procedure acts as a function approximator, whose objective is to replace the parameters on the mathematical model by their estimated values and then compute the TIM speed and current curves. Such curves are then compared with the input signals, allowing an optimized approximation. Some applications of DE can be found in similar papers [19–22]. The DE algorithm presents several advantages in comparison to other heuristic algorithms such as robustness, since broad boundary values can be considered by the algorithm, and the inherent ability of escaping from local minima [25].

3. Differential evolution

Differential evolution (DE), developed by Storn and Price in 1995 [26], is an heuristic method, based on an iterative process, whose objective is to determine approximate solutions for combinatorial optimization problems [27]. Techniques based on DE the algorithm are known for being capable of returning feasible solutions for complex and large-scale problems with low computational costs [28], being considered more efficient than other heuristics.

In the present paper, the use of the DE algorithm to estimate the electrical parameters of the equivalent circuit, as well as the moment of inertia and the friction coefficient of the induction motor is proposed.

The DE is categorized as a population-based algorithm, since it deals with a set of possible solutions in order to find the desired solution. During the process, if such a solution is still not found, the population goes through a mutation process, followed by a crossover; as a consequence, the population tends to the desired solution.

The algorithm starts with the creation of an initial population, corresponding to the first set of solutions resultant from a random selection of individuals contained in a bounded search region. The

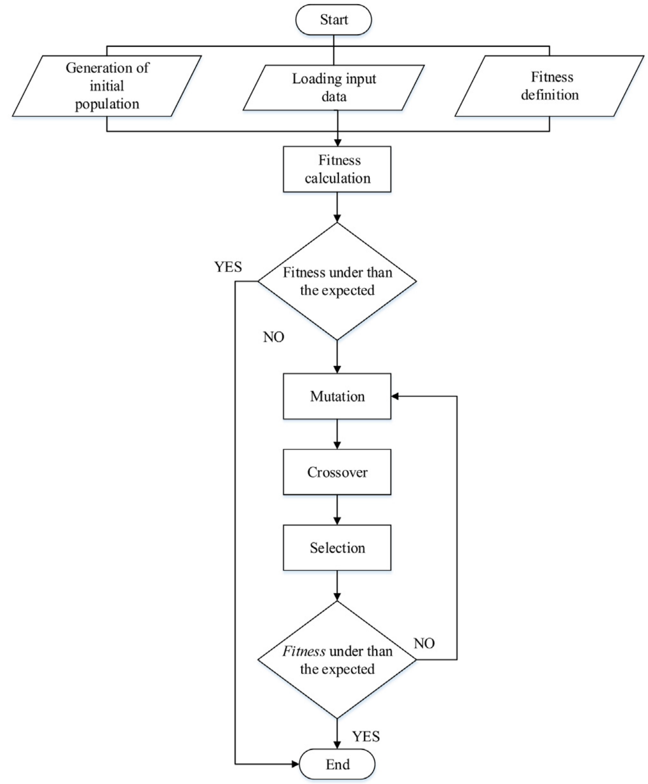

Fig. 1. DE process.

fitness function of each solution is then calculated, which corresponds to the objective function to be minimized. Three or more individuals from the initial population are then randomly selected to undergo a mutation process (three individuals are used in this paper). In this step, the vectorial difference between the second and the third individual is determined and then multiplied by a weighting factor; the result is then added to the first individual, generating the first individual of the mutated population, as presented in Eq. (12):

$$v_{i,G+1} = x_{r_1,G} + F \cdot (x_{r_3,G} - x_{r_2,G}) \tag{12}$$

where $v_{i,G+1}$ is the ith element of the mutated population, F is the weighting factor applied to the vectorial difference and $x_{r_1,G}$, $x_{r_2,G}$ and $x_{r_3,G}$ are the chromosomes randomly chosen from the population prior to mutation.

After the mutation, the crossover step begins. During the crossover, the individuals of the initial population, named target vector, are combined with the mutated population. A random number between 0 and 1 is assigned to each chromosome element, both for the target vector and for the mutated population, and this number is compared to the crossover rate, which is also a value ranging from 0 to 1 corresponding to the crossover probability of an individual of a certain population. If the assigned value is lower than the crossover rate, then the gene of the mutated population is chosen, otherwise the target vector gene is selected.

Subsequently, the fitness values of the individuals resultant from the crossover operation are calculated and compared with their respective individuals on the target vector. Finally, a new selection stage is executed, where the best individual of each comparison will be part of the next generation. The process repeats until the stop criterium, defined a priori, is met. Fig. 1 presents a simplified flowchart of the DE process.

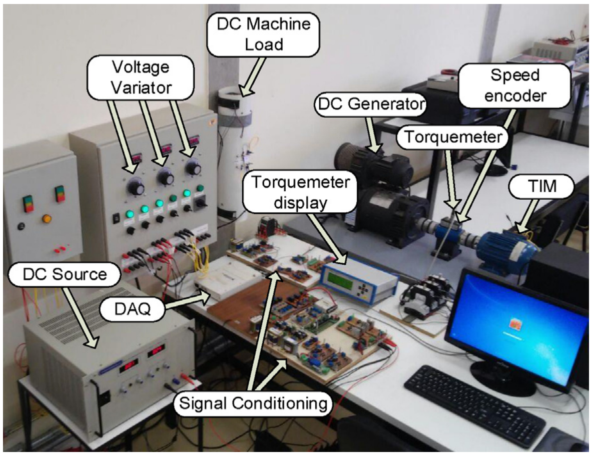

Fig. 2. Experimental workbench of the Intelligent Systems Laboratory of UTFPR.

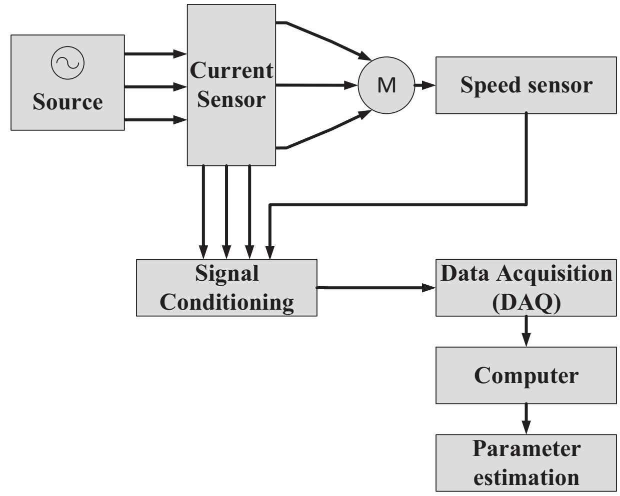

Fig. 3. Parameters estimation block diagram.

4. Methodology

The electrical and mechanical parameters of the TIM are essential not only for the efficiency analysis, but also for the development of appropriate controllers. In this sense, the search for robust parameters estimation methods with low computational cost is considerably interesting for scientific researches. The use of the DE algorithm for estimating such parameters is important to generate a computational alternative considered robust when compared to other approaches, since such optimization method allows the use of a broad search space, comprising parameters belonging to several power levels.

The motor parameters to be estimated are: stator and rotor resistances (R_1 and R_2), stator and rotor leakage inductances ($l_{\sigma 1}$ and $l_{\sigma 2}$), magnetizing inductance (L_H), moment of inertia (J) and friction coefficient (K_D). For this, we developed a function approximator algorithm using a differential evolution technique. The proposed algorithm is developed using MATLAB, which is a versatile and robust software that can be successfully used as an auxiliary simulation tool on several engineering areas, as presented, for instance, in [29–32].

4.1. Experimental structure

The input signals were obtained from an experimental testing using a 1-HP motor, 4 poles, 60 Hz and 220 V, connected in a Y configuration. The workbench used, presented in Fig. 2, is designed for monitoring voltage, current, vibration, torque and speed of a three-phase induction motor. The signal conditioning of the Hall sensors allows the phase voltages and currents to be sent to the analogic inputs of the data acquisition board. The workbench contains an induction motor coupled to a Direct Current Generator (DCG) with 2 kW, 250 V of nominal field voltage and 250 V of nominal armature voltage, granting the acquisition of digital or analogical signals lower than 50 Nm and 7000 rpm. Fig. 3 illustrates the block diagram of the estimation process.

4.2. Parameters estimation

The main objective of the present paper is to estimate electrical and mechanical parameters of the induction motor, considering three different sets of inputs: (i) current signal of one phase with the speed measured by a tachogenerator, (ii) current signal of one phase with the speed measured by a torquemeter, and (iii) just the current signal of one phase. Thus, it is possible to perform an analysis to verify the most suitable methodology for estimating the parameters. The speed was measured using two sensors with different resolutions, where the tachogenerator presents a higher resolution than the torquemeter. The current phase chosen does not make difference for the experiments, since the machine is symmetric and fed with balanced voltages.

The DE algorithm is executed as an offline procedure. The first population is randomly generated, and different boundaries are established for each parameter to be estimated. Each chromosome corresponds to a vector containing the considered parameters. After the computation of the initial population, each parameter contained in the chromosome is applied to the motor dynamic model for the calculation of the current and speed signals associated with the chromosome. Such signals are then compared with the measured signals, allowing an evaluation of the quality of the corresponding parameters.

The fitness function, when only the current signal is used, is computed using the minimum square error shown in Eq. (13), where I_i and $\hat{I}_i$ are the measured and the estimated current signals, respectively, and N is number of samples used in the fitness function.

$$fitness = \frac{1}{N}\sum_{i=1}^{N}\left(\frac{I_i - \hat{I}_i}{I_i}\right)^2 \tag{13}$$

For the cases where the speeds were also used as inputs to the algorithm, the speed portion is added to the fitness function, as presented in (14), where ω_i and $\hat{\omega}_i$ are the measured and estimated speeds, respectively. Therefore, only one fitness function is considered for each case.

$$fitness = \frac{1}{2N}\sum_{i=1}^{N}\left(\left(\frac{I_i - \hat{I}_i}{I_i}\right)^2 + \left(\frac{\omega_i - \hat{\omega}_i}{\omega_i}\right)^2\right) \tag{14}$$

The linear/non-linear least squares techniques are the most used approaches for curve fitting since they present good results, as shown in [33–35]. However, such techniques could require the use of weighting factors if the approximated quantities have different magnitudes and compound a unique objective function. In this work, the quantities in the objective function are normalized, avoiding the use of weighting factors, once we desire that both quantities have the same weight. As a consequence, the proposed technique has also yielded good results, and hence it is reasonable to assume the results are very close to the ones obtained from the aforementioned traditional techniques. Since the number N of signal samples and the amount of individuals influence the computational time of each iteration, some tests were performed to

Table 1
Parameters boundaries.

R_1 (Ω)	[1 15]
$l_{\sigma 1}$ (mH)	[0.001 0.5]
R_2 (Ω)	[2 15]
$l_{\sigma 2}$ (mH)	[0.001 0.5]
J	[0.005 0.08]
K_D	[0.0001 0.008]
L_H	[0.1 1.5]

Table 2
Convergence data for all three input cases considered.

Case	Generations	Time (min)	Best initial fitness	Best final fitness
Case 1	30	147.3	2.6371	0.002670
Case 2	28	137.5	2.5685	0.002124
Case 3	18	54.3	2.2712	0.002083

determine proper values for such parameters. After such tests, it was chosen a population with 15 individuals for all the experiments. The choice of the weighting factor and crossover rate, both ranging from 0 to 1, is also extremely important for the DE method. The higher the weighting factor, the lower the chance for the algorithm to stop in a local minimum. Therefore, initially the weighting factor is chosen to be close to 1 and, as the fitness function approximates to the desired value, the factor is reduced to a value close to 0, so the search is concentrated on the aimed region. In this paper, after numerous tests, the weighting factor was chosen to be initially equal to 0.8, decreasing to 0.2 when the final condition is attained. Concerning the crossover rate, a value of 0.5 is established to guarantee an equal probability of choosing either the target vector or the mutated vector. Since only one current is used, it is recommended to certify that the machine feeding is balanced, in order to reduce the uncertainties related to the estimated parameters. It is also important to perform the test without any load, to guarantee that the dynamic condition, which influences the mechanical parameters estimation, is not affected. However, if there is no possibility of performing a no-load test, it is important to know the torque applied to the machine.

All the tests have been performed in an Intel i7, 2.4 GHz, 8 GB RAM, Windows 8 64 bits, using Matlab 2013a.

5. Experimental results

The results are divided in two parts: induction motor parameters estimation and validation of the results. For the first part, three estimations were performed, each of which considering a different set of the input signals. The best results were used for the validation.

A broad search space was used for all the considered cases, as presented in Table 1, generating a high parametric uncertainty. On the other hand, the proposed strategy can estimate the parameters for motors with distinct power levels.

The three input cases considered are: phase A current and the speed measured from a tachogenerator (Case 1), phase A current and the speed measured from a torquemeter (Case 2), and only the phase A current (Case 3). The stopping criterion established for all cases is a fitness value lower than 0.003, since prior experiments have shown that, when such is attained, the error between the estimated and experimental curves is lower than 5%, mainly on steady state, both for the speed and current signals. A second stopping criterion adopted is the maximum number of generations, in order to limit the processing time of the algorithm. In this paper, it is defined a maximum of 50 generations, however such maximum has not been reached in the performed simulations. Table 2 presents the convergence data for each considered case.

Table 3
Parameters estimated from the phase A current and from the speed measured by the tachogenerator. The resistances are given in Ω, and the inductances, in mH.

Parameter	R_1	$l_{\sigma 1}$	R_2	$l_{\sigma 2}$	J	K_D	L_H	Fitness
Result	3.6527	0.0477	5.2438	0.0043	0.0281	0.0009	0.4545	0.002670

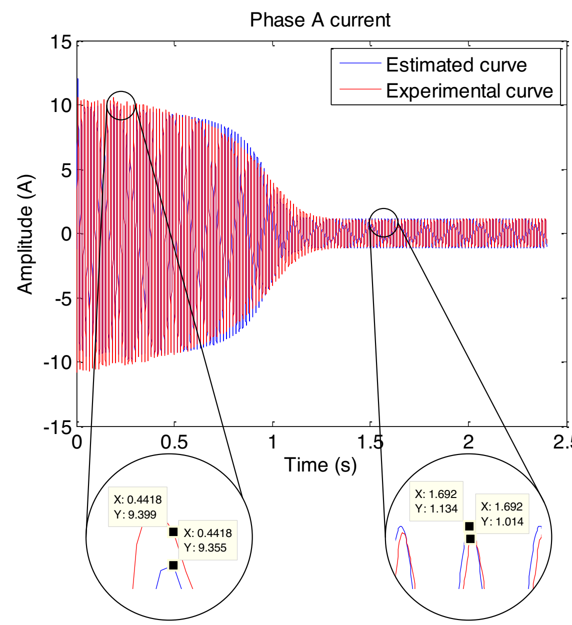

Fig. 4. Comparison of the estimated and experimental currents.

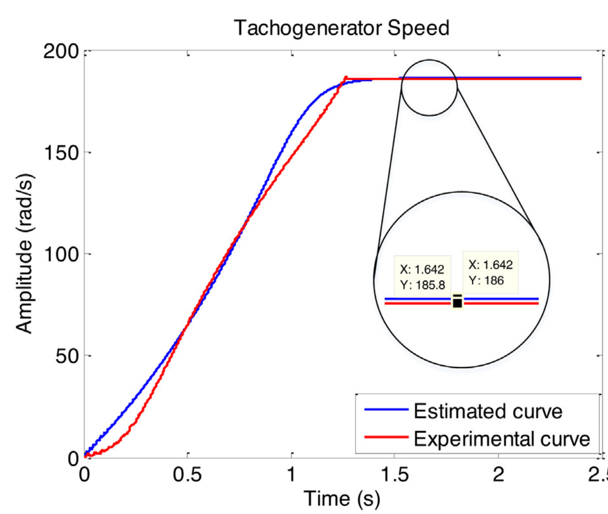

Fig. 5. Comparison of the estimated and experimental speeds, measured by the tachogenerator.

The use of the three experiments allowed for the comparison of the obtained results, as well as for the verification of the necessity of using the speed signal for parameter estimation. It is important to highlight that all the input signals were generated in the same experimental setting, guaranteeing a proper comparison of the estimation methods.

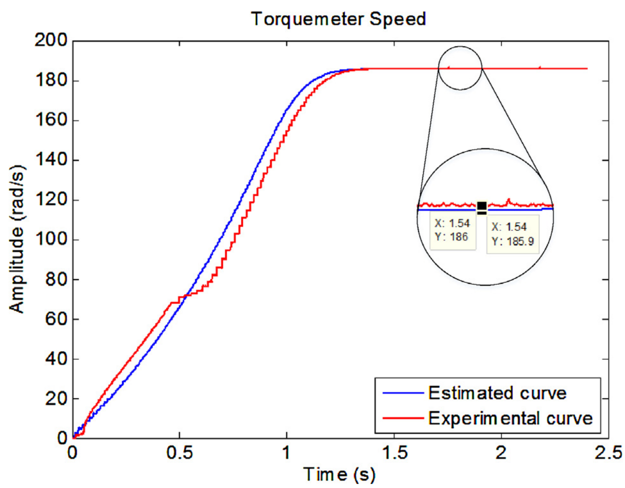

Fig. 6. Comparison of the estimated and experimental speeds, measured by the torquemeter.

Table 4
Parameters estimated from the phase A current and from the speed measured by the torquemeter. The resistances are given in Ω, and the inductances, in mH.

Parameter	R_1	$l_{\sigma 1}$	R_2	$l_{\sigma 2}$	J	K_D	L_H	Fitness
Result	3.1753	0.0405	5.6995	0.0053	0.0281	0.0013	0.5012	0.002124

5.1. Three-phase induction motor parameter estimation

5.1.1. Case 1: Phase A current and the speed measured from a tachogenerator

The best fitness results are shown in Table 3. Figs. 4–6 present, respectively, both the estimated and the experimental phase A current, as well as the speed signals measured using the tachogenerator and the torquemeter, compared with the computed estimated value.

From Fig. 4, it is possible to verify the similar behavior of both currents. It is also possible to verify, on the transient, a difference of 0.47% between the experimental and estimated curves. Concerning the steady state of the speed curves, there is a difference of 0.05% between the experimental and estimated data, both using the torquemeter and the tachogenerator.

5.1.2. Case 2: Phase A current and the speed measured from a torquemeter

For the second case, the speed is measured using the optical encoder in the torquemeter. The resolution of such sensor is lower when compared to the tachogenerator, justifying the divergent behavior observed on the transient signals.

Table 4 presents the computed results with the best fitness. Fig. 7 presents a comparison of the estimated and experimental phase A currents, and Figs. 8 and 9 present the comparison of the measured speeds, both using the tachogenerator and the torquemeter, and their estimated values.

A comparison between the presented methods shows that both yielded good results. Analysing the results from the second method, one can see that the error between the estimated and experimental currents was approximately 3% during the transient and, for the steady state speed, the percentual difference was 0.15%.

5.1.3. Case 3: Input signal – phase A current

In order to verify the importance of the speed signal in the parameter estimation procedure, only the phase A current signal is used as input for the third case. Table 5 presents the results obtained with the best fitness values. Fig. 10 displays a comparison between

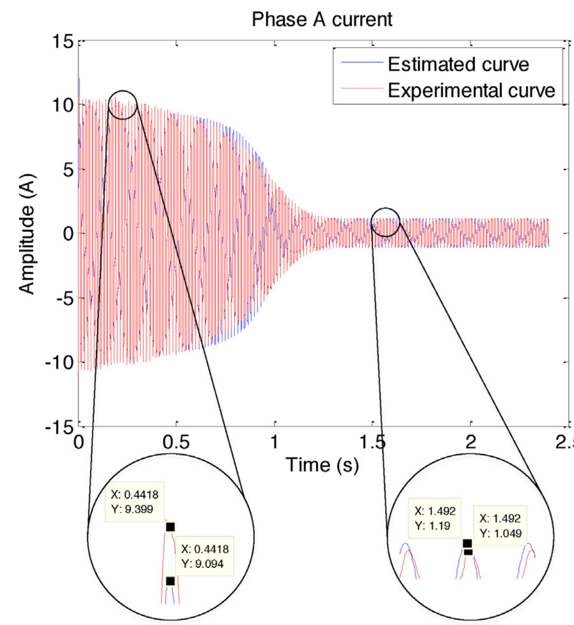

Fig. 7. Comparison of the estimated and experimental currents.

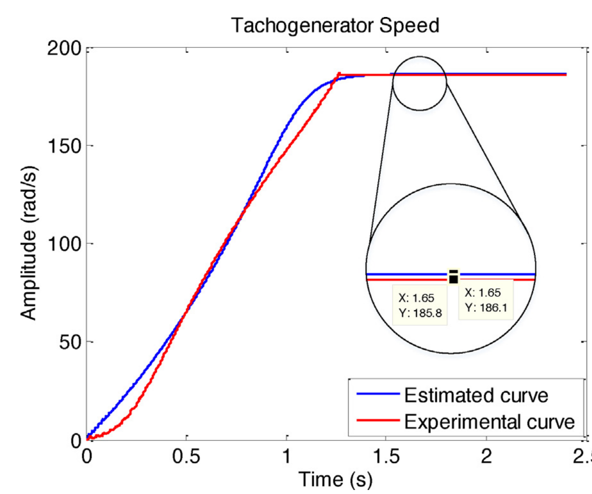

Fig. 8. Comparison of the estimated and experimental speeds, measured by the tachogenerator.

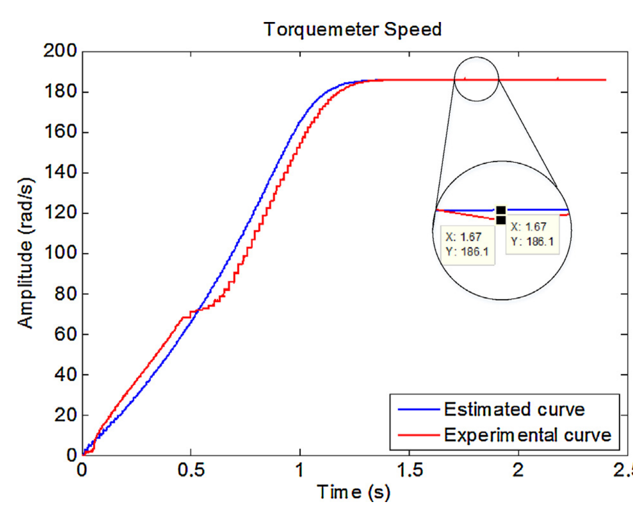

Fig. 9. Comparison of the estimated and experimental speeds, measured by the torquemeter.

Table 5
Parameters estimated from the phase A current. The resistances are given in Ω, and the inductances, in mH.

Parameter	R_1	$l_{\sigma 1}$	R_2	$l_{\sigma 2}$	J	K_D	L_H	Fitness
Result	5.0798	0.0311	4.2047	0.0202	0.0216	0.0002	0.4705	0.002083

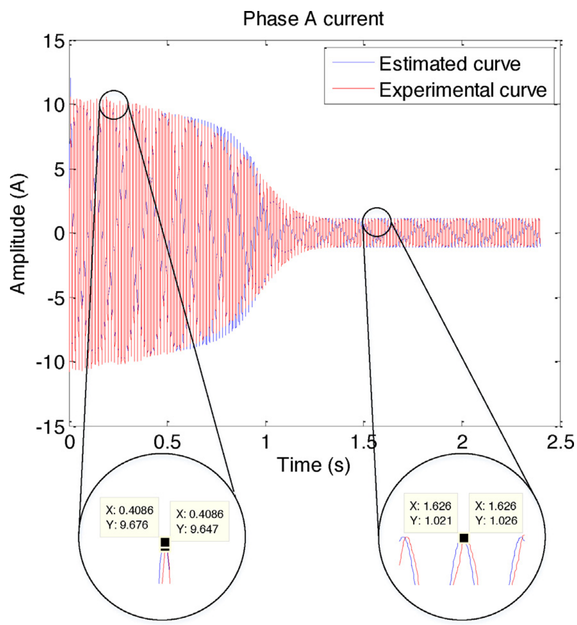

Fig. 10. Comparison of the estimated and experimental currents.

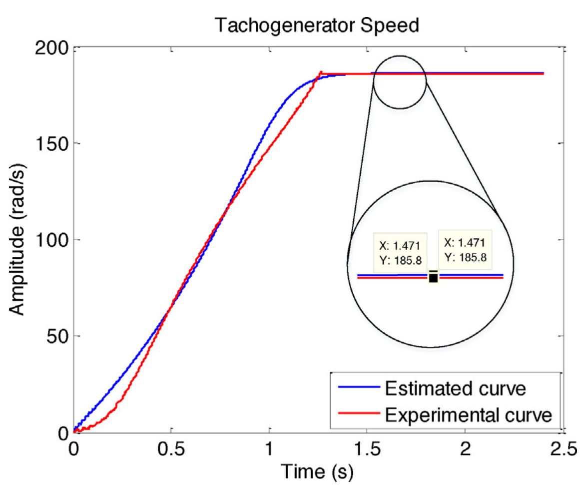

Fig. 11. Comparison of the estimated and experimental speeds, measured by the tachogenerator.

the estimated and the experimental current signals. Although no speed sensor was used for the estimation, Figs. 11 and 12 present the speed measured by the tachogenerator and by the torquemeter, respectively, along with the estimated speed, allowing for an evaluation of the estimation efficiency using only the current signal.

After performing an analysis of the speed signals, one can note a difference between the generated and the measured signals during the transient, which occurs due to the different resolutions of the speed sensors. If only the current signal is used as input, the difference between the estimated and experimental speeds is approximately 0.5%. Moreover, in this case, the interferences in the speed data acquisition have no influence on the parameters estimation method proposed in this paper. Note also that the difference

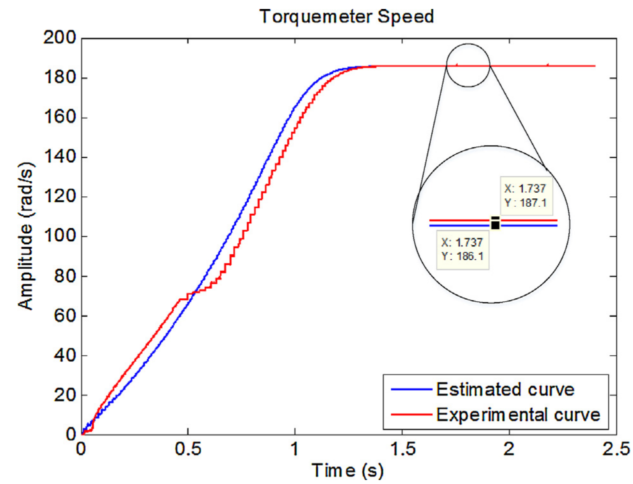

Fig. 12. Comparison of the estimated and experimental speeds, measured by the torquemeter.

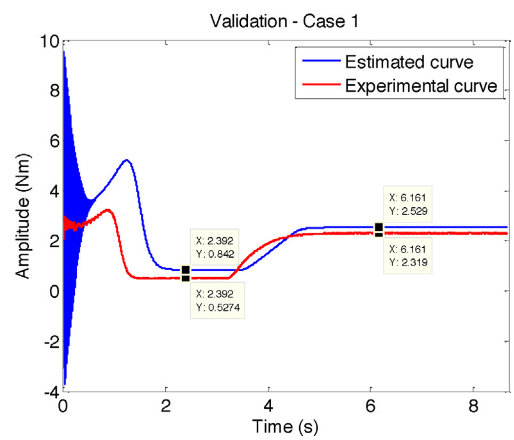

Fig. 13. Validation of the method using the phase A current and the speed measured from the tachogenerator as an input signal.

between the estimated and the experimental steady state currents is also approximately 0.5%.

5.2. Validation

For the validation of the proposed method, an input load test was performed. Initially, the motor torque was given by 0.5 Nm, provided by the direct current motor coupled by the shaft to the induction motor; after a period of 3.5 s, a torque of 2.3 Nm was then applied. The first validation was with Case 1, which is the estimation using the phase A current and the speed measured from a tachogenerator, and the result is presented in Fig. 13. The difference between the experimental and the estimated signal at steady state was about 9%, which is considered satisfactory.

The second validation was performed with Case 2, which consists of using the phase A current and the speed measured by the torquemeter as input signals of the DE algorithm. The validation is presented in Fig. 14. Note that the steady state error, with a load, corresponds to 6%, indicating that the use of the torquemeter optical encoder, even with lower resolution, yields a similar estimation when compared to the measurement with the tachogenerator.

The last validation, presented in Fig. 15, was performed for Case 3, using only the phase A current as input signal. For this case, the percentage error between the estimated and computed signals, also at steady state with load, is given by 0.13%.

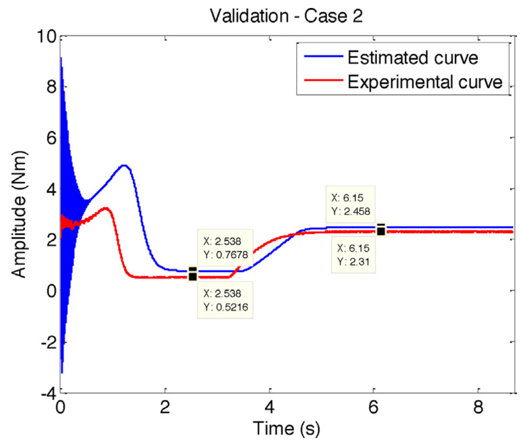

Fig. 14. Validation of the method using the phase A current and the speed measured from the torquemeter as an input signal.

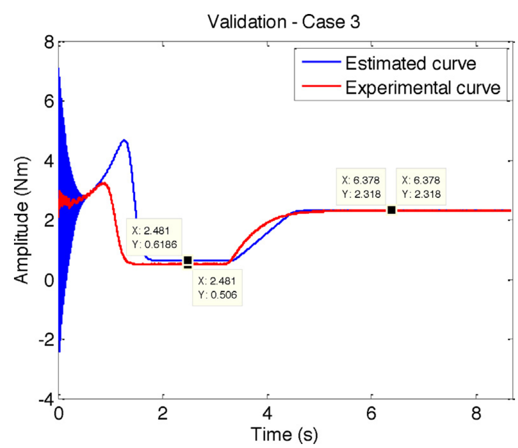

Fig. 15. Validation of the method using the phase A current as an input signal.

Through a comparative analysis of the three validation processes, it can be observed that Case 3, which used only the current signal, presents a lower percentage error during the validation, at steady state, when compared to other situations. Additionally, the linear model developed and presented in this paper disregards nonlinearities, such as skin effect and electromagnetic saturation. As a consequence, discrepancies between the measured data and those obtained through simulations can be observed during the transient. However, once the steady state is attained, one can verify the similarity of the computational model compared to the experimental measurements. In particular, it is important to highlight the information presented in Fig. 15 as one of the contributions of the paper, which considers the curve estimated with the phase A current as input signal of the proposed system at steady state. Still, the authors applied a low frequency load step to test the robustness of the method when the machine is subject to torque disturbances. According to Figs. 13–15, it can be verified that the parameters estimated from the proposed method reproduce the machine behavior assessed through experimental tests.

The following section presents a comparison between Case 3 of the present paper with other similar papers in the literature.

5.3. Comparison of results

A comparative analysis of the results obtained from Case 3 of the proposed paper, and of other works in the literature, is performed in the sequence. Table 6 presents a comparison of the parameters estimated, as well as the input signals used, in three other papers

Table 6
Comparison with other similar works in the literature.

Work		This work	[17]	[18]	[19]
Method	DE	PSO	GA	DE	
Input	Voltage	NO	NO	YES	YES
	Current	YES	NO	YES	YES
	Speed	NO	YES	NO	YES
	Torque	NO	YES	NO	YES
Parameter	R_1 (Ω)	YES	YES	YES	YES
	R_2 (Ω)	YES	YES	YES	YES
	$l_{\sigma 1}$ (mH)	YES	YES	YES	YES
	$l_{\sigma 2}$ (mH)	YES	YES	YES	YES
	L_m	YES	YES	YES	NO
	J	YES	NO	YES	NO
	K_D	YES	NO	YES	NO

[17–19], which are based on the implementation of the PSO, GA and DE optimization methods.

The main advantage of the proposed work, when compared to [17–19], is the use of only one current signal for parameter estimation. Furthermore, seven parameters of the induction motor are estimated.

The method presented in [18] is similar to the technique proposed in this paper, with the difference that the compared method uses the voltage as input signal, and no validation is performed to certify the performance.

6. Conclusion

A method for parameters estimation of a three-phase induction motor, using a DE algorithm, is proposed in this paper. The method consists of using the DE algorithm to estimated the parameters by minimizing the difference between the measured signals and the outputs of a linear model for the motor. Three experiments were then performed in order to compare the quality of the parameter estimation when considering different signals and sensors. Analyzing the results, a small variation among the values resultant from the three types of experiment used can be observed.

The strategies that included the speed in the input signal were developed to properly analyze the technique that only considers the current for input signal. It was not necessary to use the speed information to estimate the parameters, whose measurement requires more sophisticated sensors.

Through the analysis performed in the validation section, it is clear that the best result was the estimation using only the current as input signal, where the difference between the experimental and estimated torque was of 0.13%, at steady state.

It is also important to highlight that the DE algorithm presents the advantage related to the search space. In this paper, a broad range of each parameter was considered; nevertheless, the convergence of the algorithm was satisfactory, attesting the robustness of the method.

Acknowledgments

We would like to thank the financial support provided by the Conselho Nacional de Desenvolvimento Científico e Tecnológico – CNPq (Processes # 474290/2008-5, 473576/2011-2, 552269/2011-5), to the Fundação Araucária de Apoio ao Desenvolvimento Científico e Tecnológico do Paraná (Process # 06/56093-3) e to the Capes-DS scholarship.

References

[1] I.L. Sauer, H. Tatizawa, F.A. Salotti, S.S. Mercedes, A comparative assessment of Brazilian electric motors performance with minimum efficiency standards, Renew. Sustain. Energy Rev. 41 (2015) 308–318.
[2] M. Al-Badri, P. Pillay, P. Angers, A novel in situ efficiency estimation algorithm for three-phase IM using GA, IEEE method F1 calculations, and pretested motor data, IEEE Trans. Energy Convers. 30 (3) (2015) 1092–1102.
[3] G. Cui, L. Liu, S. Li, P. Yang, F. Yang, L. Chen, J. Dong, Optimization design of high efficiency variable frequency induction motor based on finite element analysis, 17th International Conference on Electrical Machines and Systems, ICEMS 2014 (2015) 701–705, http://dx.doi.org/10.1109/ICEMS.2014.7013559.
[4] C.T. Raj, S.P. Srivastava, P. Agarwal, Energy efficient control of three-phase induction motor – a review, Int. J. Comput. Electr. Eng. 1 (1) (2009) 61–70.
[5] N. Popov, S. Vukosavic, E. Levi, Motor temperature monitoring based on impedance estimation at PWM frequencies, IEEE Trans. Energy Convers. 29 (1) (2014) 215–223.
[6] M.A. Jirdehi, A. Rezaei, Parameters estimation of squirrel-cage induction motors using ANN and ANFIS, Alex. Eng. J. 55 (1) (2016) 357–368.
[7] H. Kojooyan-Jafari, L. Monjo, F. Córcoles, J. Pedra, Parameter estimation of wound-rotor induction motors from transient measurements, IEEE Trans. Energy Convers. 29 (2) (2014) 300–308.
[8] F. Duan, R. Živanović, S. Al-Sarawi, D. Mba, Induction motor parameter estimation using sparse grid optimization algorithm, IEEE Trans. Ind. Inf. 12 (4) (2016) 1453–1461.
[9] Y. Horen, P. Strajnikov, A. Kuperman, Simple mechanical parameters identification of induction machine using voltage sensor only, Energy Convers. Manag. 92 (1) (2015) 60–66.
[10] T. Ameid, A. Menacer, H. Talhaoui, I. Harzelli, Rotor resistance estimation using Extended Kalman filter and spectral analysis for rotor bar fault diagnosis of sensorless vector control induction motor, Measurement (2017).
[11] IEEE Standard Test Code for Resistance Measurement, IEEE Std 118-1978, 1978, pp. 1–20.
[12] M. Jirdehi, A. Rezaei, Parameters estimation of squirrel-cage induction motors using ANN and ANFIS, Alex. Eng. J. 55 (1) (2016) 357–368.
[13] A. Bechouche, H. Sediki, D. Ould Abdeslam, S. Haddad, A novel method for identifying parameters of induction motors at standstill using ADALINE, IEEE Trans. Energy Convers. 27 (1) (2012) 105–116.
[14] L. Monjo, H. Kojooyan-Jafari, F. Corcoles, J. Pedra, Squirrel-cage induction motor parameter estimation using a variable frequency test, IEEE Trans. Energy Convers. 30 (2) (2015) 550–557.
[15] Y. Horen, P. Strajnikov, A. Kuperman, Simple mechanical parameters identification of induction machine using voltage sensor only, Energy Convers. Manag. 92 (2015) 60–66.
[16] F. Stinga, A. Soimu, M. Marian, Online estimation and control of an induction motor, in: 19th International Conference on System Theory, Control and Computing, ICSTCC, 2015, pp. 742–746.
[17] V. Sakthivel, R. Bhuvaneswari, S. Subramanian, Multi-objective parameter estimation of induction motor using particle swarm optimization, Eng. Appl. Artif. Intell. 23 (3) (2010) 302–312.
[18] E. Boudissa, M. Bounekhla, Genetic algorithm with dynamic selection based on quadratic ranking applied to induction machine parameters estimation, Electr. Power Compon. Syst. 40 (10) (2012) 1089–1104.
[19] M. Arslan, M. Çunkaş, T. Sağ, Determination of induction motor parameters with differential evolution algorithm, Neural Comput. Appl. 21 (8) (2012) 1995–2004.
[20] J.J. Guedes, M.F. Castoldi, A. Goedtel, Temperature influence analysis on parameter estimation of induction motors using differential evolution, IEEE Lat. Am. Trans. 14 (9) (2016) 4097–4105, http://dx.doi.org/10.1109/TLA.2016.7785939.
[21] T. Banerjee, J. Bera, G. Sarkar, Parameter estimation of three phase induction motor using gravitational search algorithm for IFOC, in: Michael Faraday IET International Summit 2015, 2015, pp. 607–610.
[22] R.K. Ursem, P. Vadstrup, Parameter identification of induction motors using differential evolution, in: The 2003 Congress on Evolutionary Computation, 2003 CEC ‘03, vol. 2, 2003, pp. 790–796.
[23] P.C. Krause, O. Wasynczuck, S.D. Sudhoff, Analysis of Electrical Machinery and Drive Systems, 2nd ed., John Wiley and Sons, 2002.
[24] C.-M. Ong, Dynamic Simulation of Electric Machinery: Using MATLAB/SIMULINK, vol. 5, Prentice Hall – PTR, Upper Saddle River, NJ, 1998.
[25] S. Das, P. Suganthan, Differential evolution: a survey of the state-of-the-art, IEEE Trans. Evolut. Comput. 15 (1) (2011) 4–31.
[26] K. Price, R.M. Storn, J.A. Lampinen, Differential Evolution: A Practical Approach to Global Optimization, Springer Science & Business Media, 2006.
[27] A. Qing, Differential Evolution: Fundamentals and Applications in Electrical Engineering, Wiley-IEEE Press, 2009.
[28] S. Bandyopadhyay, A. Mukherjee, An algorithm for many-objective optimization with reduced objective computations: a study in differential evolution, IEEE Trans. Evolut. Comput. 19 (3) (2015) 400–413, http://dx.doi.org/10.1109/TEVC.2014.2332878.
[29] M. Valipour, M.E. Banihabib, S.M.R. Behbahani, Comparison of the ARMA, ARIMA, and the autoregressive artificial neural network models in forecasting the monthly inflow of Dez dam reservoir, J. Hydrol. 476 (2013) 433–441.
[30] R. Ponalagusamy, S. Priyadharshini, Nonlinear model on pulsatile flow of blood through a porous bifurcated arterial stenosis in the presence of magnetic field and periodic body acceleration, Comput. Methods Progr. Biomed. 142 (2017) 31–41.
[31] M. Momeni, S. Yazdani, M. Khorshidi, Clustering customers by C-mean method (case study: Golestan company), Int. Bus. Manag. 10 (8) (2016) 1406–1413.
[32] M.R. Araújo, C. Pereira, A practical first-zone distance relaying algorithm for long parallel transmission lines, Electr. Power Syst. Res. 146 (2017) 17–24.
[33] K. Wang, J. Chiasson, M. Bodson, L.M. Tolbert, A nonlinear least-squares approach for identification of the induction motor parameters, IEEE Trans. Autom. Control 50 (10) (2005) 1622–1628.
[34] D.M. Reed, H.F. Hofmann, J. Sun, Offline identification of induction machine parameters with core loss estimation using the stator current locus, IEEE Trans. Energy Convers. 31 (4) (2016) 1549–1558.
[35] S.R. Shaw, S.B. Leeb, Identification of induction motor parameters from transient stator current measurements, IEEE Trans. Ind. Electron. 46 (1) (1999) 139–149.